Journal of Marine Science and Application (2025) 24: 1049-1063
https://doi.org/10.1007/s11804-025-00669-6

RESEARCH ARTICLE

Development of a ModelBuilder for Automatizing the Calculation of Coastal Vulnerability Index: Application in the Northern Corinthian Gulf

Andreas Tsokos[1], Vassiliki Tsoukala[1], Evangelos Spyrou[2], Alexandros Liaskos[2] and Niki Evelpidou[2]

Received: 17 June 2024 / Accepted: 07 September 2024

Abstract

Coasts are subject to multiple natural hazards, which are increasing nowadays. Coastal flooding and erosion are some of the most common hazards affecting coastlines. Being aware of the vulnerability of coasts is important to achieve integrated coastal management. The coastal vulnerability index (CVI) is a common index used to assess coastal vulnerability because it is easily calculated. However, given that its calculation includes numerous manual steps, it requires considerable time, which is often unavailable, to produce accurate and utilizable results. In this work, we developed a ModelBuilder model by using the tools provided by ArcGIS Pro (ESRI). Through this model, we automatized most of the steps involved in CVI calculation. We applied the ModelBuilder model in the northern Peloponnese, for which the CVI has already been calculated in three other works. We were thus able to assess the effectiveness of our ModelBuilder model. Our results demonstrated that through the ModelBuilder, most of the processes could effectively be automatized without problems, and our results are consistent with the findings of previous works in our study area.

Keywords Shoreline changes; Coastal vulnerability index; ModelBuilder; ArcGIS pro; Automatization

1 Introduction

Coastal zones are a dynamic environment that is easily affected by multiple natural and anthropogenic factors (Dronkers, 2005). As a result, they are systems that are highly vulnerable to natural hazards (Anfuso et al., 2021; Castelle et al., 2024; Lam et al., 2018; Vousdoukas et al., 2020). Low-elevation coastal areas host 10%–13% of the world's population, rendering them the most densely populated environment globally (MacManus et al., 2021). The issues of coastal erosion and rising sea levels have attracted increasing concern given that coastal zones bear a continuously increasing population and human activities, such as industry, transportation, and tourism (Ankrah et al., 2023; Bagheri et al., 2023; Dong et al., 2024; Pouye et al., 2024; Vousdoukas et al., 2020; Winckler et al., 2023).

Therefore, coastal erosion is a threat to numerous coastal areas globally (Ghanavati et al., 2023; Gracia et al., 2018; Vousdoukas et al., 2020). European countries experiencing coastal erosion include, for example, Greece (e.g., Depountis et al., 2023; Evelpidou et al., 2022), Italy (e.g., Celata and Gioia, 2024), France (e. g., Chadenas et al., 2023), Spain (e.g., Sánchez-Artús et al., 2023), Germany (Hofstede, 2024), and the U. K. (Kantamaneni et al., 2022). Coastal erosion is also present in various countries in Africa, such as Senegal, (Sarr et al., 2024), Algeria (Moradi et al., 2022), and west Africa (Dada et al., 2024); in America, such as the U.S.A. (Schuller, 2023), Costa Rica (Barrantes-Castillo and Ortega-Otárola, 2023), and Argentina (Garzo et al., 2023); and in Asia, such as Sri Lanka, Malaysia, Thailand (Saengsupavanich et al., 2023), Japan (Uda, 2022), and Indonesia (Setyawan, 2022; Tarigan et al., 2024).

Many researchers agree that climate change has already caused, and will continue causing, an increase in glacier melting and will thus aggravate the rise in sea levels (e.g., Jevrejeva et al., 2023; Vernimmen and Hooijer, 2023).

Article Highlights

- We developed a tool to calculate the Coastal Vulnerability Index automatically, using Geographic Information Systems.
- We tested and applied it in an area where it has already been calculated (manually), and it worked successfully.
- Thus, it can be used to calculate it for other areas, regardless of local conditions, saving researchers time and effort.
- This index can be used in estimating coastal vulnerability and thus facilitate coastal management.

✉ Niki Evelpidou
evelpidou@geol.uoa.gr

[1] National Technical University of Athens, Department of Civil Engineering, Laboratory of Harbor Works, Athens 15780, Greece

[2] National and Kapodistrian University of Athens, Department of Geology and Geoenvironment, Athens 15784, Greece

Coastal erosion can occur even in areas that were not previously threatened (Stockdon et al., 2023). A general consensus exists that due to climate change, wave activity will also increase, leading to increased coastal erosion problems globally (Dong et al., 2024; Patra et al., 2023; Tadesse et al., 2022). Among the most important impacts of coastal erosion and the future rise in sea levels are the losses of coastal property, coastal resilience, biodiversity, economy, and tourism; the destruction of natural habitats; land changes; damage to cultivation; and an increase in the cost of coastal management measures (Garola et al., 2022; González Rodríguez et al., 2024; Kirezci et al., 2023; Pouye et al., 2024). Quantitative assessments and analyses of coastal vulnerability appear to be necessary (Maanan et al., 2018). Spatially assessing the vulnerability of coasts to erosion can aid in decision making and adaptation strategies (Liu and Zhang, 2023; Roukounis et al., 2023; Tsaimou et al., 2023).

Coastal zones are among the most important physical parameters of coastal vulnerability to various hazards (storms, coastal erosion, coastal inundation, and tsunamis) (Pendleton et al., 2010). Coastal vulnerability refers to the susceptibility of people and infrastructure to coastal changes as a result of climate-induced coastal hazards (McLaughlin et al., 2010; Ramieri et al., 2011). Therefore, coastal vulnerability is composed of two aspects, each one of which has a different set of parameters: social (Ramieri et al., 2011) and physical (McLaughlin et al., 2010).

Several methods for assessing coastal vulnerability have been developed (cf. Liu and Zhang, 2023). For example, in some published studies, the assessment was based on physical parameters such as land use, wave characteristics, and shoreline change rates (Ahmed et al., 2018; Jana and Bhattacharya, 2013). In other cases, coastal vulnerability was assessed in combination with hazards and exposure (Merlotto et al., 2016; Narra et al., 2017; Thakur and Mohanty, 2023). A widely employed method is the use of the coastal vulnerability index (CVI) (e.g., Charuka et al., 2023; Depountis et al., 2023; Dike et al., 2024; Liu and Zhang, 2023; Ramnalis et al., 2023; Tarigan et al., 2024; Tsaimou et al., 2023).

A main advantage of the CVI is its simple functionality and easy usage. Moreover, the CVI combines the sensitivity of coastal zones to sea level changes, which are reflected by their natural properties, such as morphological inclination and wave action, with their adaptability to potential changes. After its initial introduction by Gornitz et al. (1991), the CVI was later modified by several researchers to include additional parameters (Church and White, 2011). Roukounis and Tsihrintzis (2022) have reviewed this index and the parameters used in its calculation in detail. This index is calculated by using several physical parameters, which could be geological and geomorphological. The most commonly employed factors include geomorphology, coastal slope, sea level changes, shoreline displacement, mean significant wave height, and tidal range (Gornitz et al., 1991; Hamid et al., 2021; Pendleton et al., 2005).

Geomorphology parameters refer to the geomorphological characteristics of coastal zones. They quantify the resistance of different types of coasts to a specific coastal hazard (e.g., coastal erosion) (Suhana et al., 2016; Thieler and Hammar-Klose, 1999). It is one of the parameters that affect the CVI the most (Koroglu et al. 2019; Tarigan et al. 2024). Shoreline displacement refers to the extent to which coasts have been subjected to erosion or shoreline progression: the higher the extent of the displacement, the higher the coastal vulnerability (Gornitz et al., 1991; Pendleton et al., 2005). In terms of slope, coasts of small inclination are affected by marine processes (e.g., waves and tides) to a greater extent than steeper ones (Thieler and Hammar-Klose, 1999).

The mean significant wave height quantifies the ability of waves to redistribute coastal sediments and thus provoke or hinder coastal erosion (e.g., Moradi et al., 2022; Pang et al., 2023). The tidal range is the fluctuation of the sea level due to the rotation of the sun and moon (Diez et al., 2007). It is a crucial aspect of coastal vulnerability (Fok, 2012). Generally, coastal vulnerability increases as the tidal range increases (Doukakis, 2005). Finally, sea level changes refer to the relative fluctuations in sea levels. Given that this index refers to the human lifetime scale, it only rarely consists of fluctuations; depending on the local tectonic regime, it can be considered as the relative rise, fall, or stability of sea levels (Pendleton et al., 2005). Areas with considerable sea level changes show high vulnerability (Mohd et al., 2019; Pendleton et al., 2010).

A major disadvantage of the CVI is that it requires numerical data for parameters that cannot be easily quantified. Therefore, the values of these parameters are quantified arbitrarily by researchers on the basis of their experience and knowledge of the study area, as well as the availability of data. Nevertheless, it is an accurate index for spatial studies on the vulnerability of coasts to sea level rises (European Commission, 2004; Mohanty et al., 2017).

In this study, a ModelBuilder model was developed to calculate the CVI automatically by using the ArcGIS Pro by Esri in reference to Pendleton et al. (2005). The calculation of the CVI requires numerous manual processes and a good knowledge of geomorphology. Moreover, the usage of a geographic information system (GIS) appears to be necessary. Therefore, the calculation of the CVI is a time-consuming process. Moreover, when done manually, it can lead to numerous inaccuracies. On small scales, these inaccuracies may lead to considerable modeling failure. Hence, the ModelBuilder model was constructed in such a way that it could divide the studied coastline into segments, each one of which would be assigned an integral value (1–5) for each of the six addressed parameters of the CVI on the

basis of bibliographical references. Moreover, the ModelBuilder model was developed so that it also calculates the CVI on the basis of these values. We applied this ModelBuilder model to a part of the Corinthian Gulf because at least three previous works have calculated the CVI of this area. Given that our purpose is not to assess the area's vulnerability, we used already existing results to test our model.

GIS has grown to be a powerful tool for modeling (Buhmann et al., 2002; Maguire et al., 2005) and can hence be used for future predictions (Goodchild, 2005). An advantage offered by the ArcGIS (or ArcMap) ModelBuilder is that it can combine different GIS operations while running models that are composed of different databases (Pfaff and Glennon, 2004). Moreover, it can simplify and accelerate modeling (AbdelRahman and Tahoun, 2019; Csáfordi et al., 2012; Schaller and Mattos, 2010).

ModelBuilder functions as a sequence of GIS functions, each of which is performed once the previous one is completed successfully (https://pro.arcgis.com/en/pro-app/latest/help/analysis/geoprocessing/modelbuilder/what-is-modelbuilder- . htm; accessed July 17, 2024). The GIS ModelBuilder offers the ability to manage geoprocessing tools and has thus been applied in various fields of science. Several studies have utilized the ArcMap and/or ArcGIS ModelBuilder for their models. For example, Csáfordi et al. (2012) developed a ModelBuilder model to calculate the universal soil loss equation (Wischmeier and Smith, 1978), which is commonly used to model soil erosion. Chaaban et al. (2012) employed ModelBuilder to create two models to measure coastline retreat on a shore of France. Schaller and Mattos (2010) applied ModelBuilder in landscape development planning. Tiwari and Ajmera (2021) utilized ModelBuilder for land suitability assessment. AbdelRahman and Tahoun (2019) used ModelBuilder to assess soil quality. ModelBuilder has also been employed for soil quality assessment (Mohamed et al., 2011, 2015), land resource assessment (Saleh et al., 2015), drought hazard assessment (Belal et al., 2014), and solar energy modeling (Effat, 2017; Effat and El-Zeiny, 2017) in Egypt.

ModelBuilder requires three distinct elements: an input, geoprocessing tools, and an output dataset (Allen, 2011; Csáfordi et al., 2012). Input parameters are defined by the user. Although geoprocessing tools are usually predefined in accordance with GIS software, the user determines which of them will be used and in what way. Output data are produced by ModelBuilder on the basis of the other two elements. Models created through the ModelBuilder tool need to be tested in several areas to be assessed and/or corrected (Csáfordi et al., 2012). A crucial parameter to be considered when developing a ModelBuilder model is to identify the nature and type of the model(s) to be implemented, the modeling process, and how GIS will used to perform these processes (Chang, 2014). Defining the objectives of the model and dividing it into elements, wherein each element interacts properly with the others, are also important (Darwish, 2023).

The ArcGIS ModelBuilder has proven to be a useful tool in coastal zone studies (Hysa and Baskaya, 2018). It can identify the intersection between shorelines and measure coastline retreat and advance (Deabes, 2017; Kaliraj and Chandrasekar, 2012). It can be effective in quantifying changes in the shoreline (retreat or advance) (Deabes, 2017) and monitoring the impacts of the rise in sea levels (Darwish, 2023) in addition to coastal vulnerability (Chaaban et al., 2012; Kaliraj and Chandrasekar, 2012).

2 Study area

The study area is the northern-central part of the Peloponnese, Greece. Specifically, it is a 12 km part of the coastline from Sykia to the Kamari settlements, including the town of Xylokastro (Figure 1). It is located in the southern part of the Corinth Gulf.

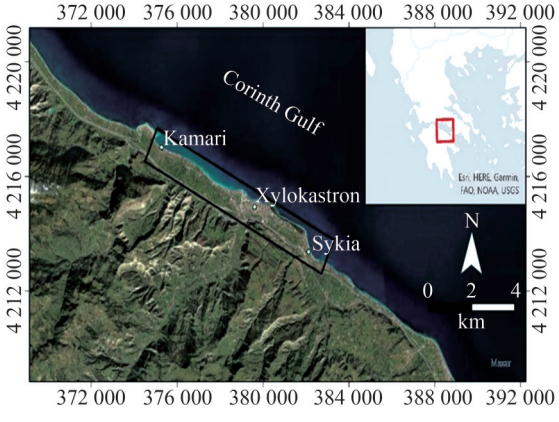

Figure 1 Satellite image of the study area and its location in Greece

As mentioned previously, the purpose of our work is not to calculate the vulnerability of the Peloponnesian coast but to develop and test our ModelBuilder model instead. This particular region was selected for two reasons: First of all, it is ideal for the application of the CVI because it is characterized by low coastal morphology and intense recent relative sea level changes (due to intense tectonic activity) and because its susceptibility to coastal erosion is well-known (Valaouris et al., 2014).

Second, three works on the coastal vulnerability of this area already exist (Karymbalis et al., 2012; Ramnalis et al., 2023; Tragaki et al., 2018). Our aim is not to assess the area's vulnerability but rather the functionality of our tool in calculating the CVI. Applying our ModelBuilder model in an area for which the CVI has already been calculated and where the effects of coastal hazards are already known and mapped has allowed us to compare our results with the findings of already existing works on the area and, there-

fore, assess the functionality of our ModelBuilder model.

2.1 Geological and geomorphological setting

The mean high tide in the study area is approximately 0.15 m relative to the sea level (Tsimplis, 1994). Northwestern winds prevail (Soukissian et al., 2007; Valaouris et al., 2014). In contrast to tides, waves can cause remarkable localized rises in the sea level surface (Hydrographic Service of the Hellenic Navy, 2005). Nevertheless, the wave height does not exceed 0.1 m (Soukissian et al., 2007).

A number of rivers and torrents flow into the Corinth Gulf, and their estuaries are located within the study area (Vassilakis et al., 2007), eroding relatively soft lithologies and thus producing considerable sediment yield (Vassilakis et al., 2016). Morphological slopes are generally less than 5% in the coastal zone, without any coastal escarpments (Vassilakis et al., 2016). Regarding the submarine geomorphology, the slope is steep in the largest part of the area.

Previous studies (Valaouris et al., 2014; Vassilakis et al., 2016) have mentioned that several sections of the study area's coastal zone have already suffered coastal erosion (see Section 2.2 for details). Coastal erosion in other sections was reported to have progressed. By correlating satellite images from the period of 1970–1996, Valaouris et al. (2014) concluded that the shoreline has advanced by up to 10 m depending on the area and has retreated by up to 23 m at other locations. For the period of 1996–2011, the study area had almost exclusively undergone a mean retreat of 14 m.

Valaouris et al. (2014) predicted the future state of the coastline of Xylokastro under the assumption that no further tectonic displacement will occur and taking into account the moderate scenario of IPCC for a 0.38 m rise in sea level in the next 100 years. They predicted that the western and eastern coasts will retreat by 10.9 and 4.1 m, respectively. Assuming a rise in sea levels of more than 1 m, the retreat on the western coast will exceed 23.8 m (Valaouris et al., 2014).

The area of the Corinthian Gulf is characterized by intense Quaternary tectonic activity (e. g., Armijo et al., 1996; Evelpidou et al., 2023; Roberts et al., 2009). The study area is controlled by north-dipping faults parallel to the shoreline, most of which are normal and active (Briole et al., 2000; Hollenstein et al., 2008). The Xylokastro fault is a dominant normal fault and has caused a high-rate tectonic uplift in the study area (Armijo et al., 1996).

2.2 Previous studies on coastal vulnerability in the study area

Karymbalis et al. (2012) applied the CVI, which they named the coastal sensitivity index (CSI). The six parameters that they incorporated are the same as those described herein, except for the parameter of shoreline displacement, which corresponded to the shoreline erosion/accretion rate rather than the measured shoreline displacement used in this work (instead of rate). They categorized the values of the CSI as very high (> 6.2), high (5–6.2), medium (3.9–5), low (1.6–3.9), and very low (< 1.6). The CSI of the area of Kamari was categorized as moderate, whereas that of the immediate southeastern part was categorized as low. Interestingly, the CSI of the area west of Xylokastro until Sykia has been categorized as low to very low.

In a recent study, Ramnalis et al. (2023) calculated the CVI, to which they added four socioeconomic factors, namely, population density, land cover, road network, and railway network. They named this index the integrated CVI and calculated it in two forms: a) as the square root of all factors to their number and b) as the sum of the physical and socioeconomic factors (individually) divided to two. In case a), the coastal vulnerability of Kamari was categorized as low, progressed gradually to high until Xylokastro, and was moderate east of it. In case b), the coastal vulnerability of Kamari was categorized as high and that of the surrounding coasts as moderate. Immediately after, the coastal vulnerability of the area was very high, then high, very high in the area of Xylokastro, and high immediately east.

Tragaki et al. (2018) performed a CVI analysis for the whole Peloponnese, including the study area. In their case, the coastal vulnerability of the whole study area was classified as moderate, except for that of Kamari, which was categorized as very high.

3 Materials and methods

3.1 Standard step method for the calculation of the CVI

The CVI was used for the assessment of the study area's vulnerability. The parameters incorporated into the CVI include three geological and three physical parameters (Karymbalis et al., 2012; Pendleton et al., 2005, 2010). The geological parameters include the following:

a. geomorphology, that is, the shore's resistance to erosion;

b. shoreline displacement, that is, the long-term trend regarding regression or progression; and

c. coastal slope, which reflects the area's vulnerability to flooding.

The physical parameters include

d. significant wave height,

e. tidal range, and

f. relative sea level change rate.

The index is given by the following equation:

$$\mathrm{CVI} = \sqrt{\frac{a \cdot b \cdot c \cdot d \cdot e \cdot f}{6}} \tag{1}$$

Although digitized Greek coastlines can be found through several platforms and official services, high-accuracy data for our small study area are not publicly accessible. Therefore, the shoreline was digitized by using Google Earth Pro. It was then inserted into ArcMap v. 10.4 and ArcGIS v. 3.2. for further processing.

The studied coastline was digitized in the form of a polyline and divided into segments. The first segmentation was performed on the basis of the geomorphology factor. Geomorphological zones were determined through the combined usage of Google Earth Pro and drone pictures accessed through TripInView.

We followed the classification by Pendleton et al. (2005): very high corresponds to low-elevation sandy beaches or estuarine mouths; high corresponds to highly engineered sections; moderate corresponds to alluvial fans and cliffs with sandy beaches; low corresponds to low-medium cliffs and rocky platforms; and very low corresponds to high vertical cliffs. In contrast to Pendleton et al. (2005), we considered gravelly or cobbly beaches as moderate rather than high because, in our case, the study area is only divided into sandy, gravelly beaches, and hard engineering (very high, medium, and very low respectively).

These segments were resegmented on the basis of the shoreline displacement factor. For example, if a segment of the coastline showed two or more zones of different values for the parameter of shoreline displacement, this segment was resegmented in accordance with these zones (Figure 2). Each segment was given a value for each of these factors. These factors ranged from 1–5, reflecting low to high vulnerability. For example, low coastal slopes would correspond to low vulnerability and were thus assigned low values. The values are shown in Table 1.

Factor *b*, shoreline displacement, was obtained through the correlation between different positions of the shoreline (Chaaban et al., 2012) and was part of previous research on the area (Vassilakis et al., 2016). Specifically, analog satellite images from the periods of 1945 (Hellenic Cadastre, 2021), 1987, 1996, and 2010 and digital satellite images from the periods of 2000 (Ikonos-2), 2008 (Ikonos-2), and

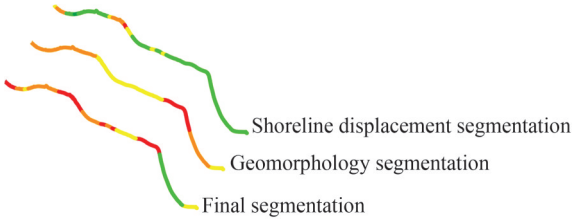

Figure 2 Segmentation of a part of the coastal zone based on geomorphology and shoreline displacement

2012 (WorldView-2) were obtained and analyzed by using photogrammetrical methods (Vassilakis and Papadopoulou-Vrynioti, 2014). Unmanned aerial vehicle pictures were also taken in the study of Tsokos (2024) on July 20, 2017; nine flights were made at a height of 120 m. All the above images were inserted into a GIS environment and georeferenced by using ArcMap 10.4 and ArcGIS v. 10 by Esri, thus allowing for digitization and correlation between older shoreline positions (Mullick et al., 2020). The coordinate system used was the Hellenic Geodetic System of Reference (HGSR/ΕΓΣΑ'87) (Mugnier, 2002). Past changes in the position of the shoreline were measured by using the Digital Shoreline Analysis System v. 4.3 extension of ArcGIS, which allows for the creation of sections perpendicular to the shoreline (Thieler et al., 2009).

Shoreline displacement ranges from −0.69 m (shoreline retreat) to +0.20 m (shoreline progression) and has been categorized as 1 for shoreline progression and 2–5 for shoreline retreat (2: 0–0.19; 3: 0.2–0.39; 4: 0.4–0.59; 5: 0.6–0.69).

The coastal slope (*c*) was obtained automatically by GIS software. A digital elevation model (DEM) with 4 × 4 accuracy was created through the digitization of the topographic diagrams by the Hellenic Military Geographical Service on a 1 : 5 000 scale. For slope categorization, we adopted the value ranges proposed by Alexandrakis et al. (2010) and measured the distance of the shoreline from the 5 m contour line. Slope values (1–5) were assigned to the slope ranges 10.0%–31.0%, 4.8%–10.0%, 3.3%–4.8%, 1.4%–2.9%, and 2.9%–3.3% on the basis of the geometric interval classification provided by ArcGIS Pro.

Table 1 CVI parameters and their values

Parameter	1	2	3	4	5
	Very low	Low	Medium	High	Very high
Geomorphology	–	–	Cobbly/gravelly beaches	roads/hard engineering	sandy beaches
Shoreline displacement (m)	progression	0–0.19	0.2–0.39	0.4–0.59	0.6–0.69
Coastal slope (%)	>12	12–9	9–6	6–3	<3
Relative sea level change	–	–	–	high uplift rates	–
Wave height	<0.1 m	–	–	–	–
Tidal range	0.15 m	–	–	–	–

Wave height and tidal range were classified as very low for the whole study area for three reasons: First, they are very low in the whole study area (Soukissian et al., 2007). Therefore, there is no need to categorize them further because they would only slightly affect the final value of the CVI. Second, both sources, as well as several online open-data platforms examined (Copernicus, 2023; Hellenic Navy Hydrographic Service, 2020; Israel Marine Data Center, n.d.; National and Kapodistrian University of Athens, 2023; National Oceanography Centre, 2023; UNESCO, 2023), lacked a detailed categorization for the study area regarding either its tidal range or wave height. Finally, this work aims not to calculate the CVI *per se* but rather to examine the efficacy of a ModelBuilder model that can calculate it automatically.

The wave height of the studied segment was also categorized as very low by Karymbalis et al. (2012), whereas Ramnalis et al. (2023) considered very low values for the tidal range and wave height for their whole coastline (i.e., the whole northern Peloponnese, including our segment). Tragaki et al. (2018) considered wave height as very low for our segment and that for the whole Peloponnesian coast as very low and equal to the tidal range.

The same is true for relative sea level changes; given the intense tectonic uplift in the area (Armijo et al., 1996), the whole study area is classified as high in terms of relative sea-level changes. Although several works have been conducted on different sites of the northern Peloponnese (e.g., Evelpidou et al., 2023; Pirazzoli et al., 1994; Turner et al., 2010), the study area has not been studied to such an extent that could allow for further categorization regarding relative sea level changes. This situation is in accordance with that in previous studies on the area. Karymbalis et al. (2012) and Ramnalis et al. (2023) have also categorized the whole studied segment as very low (in the case of Ramnalis et al. (2023), their whole coastline has been categorized as very low), whereas Tragaki et al. (2018) have considered relative sea level changes as low for the whole Peloponnesian coastline.

3.2 ModelBuilder description for the automation of CVI calculation

3.2.1 Input and preprocessing

The model was designed to process a shoreline polyline dataset, where each entry in the attribute table corresponds to a specific segment of the shoreline. This table is enriched with vulnerability data for several CVI variables. As mentioned above, these variables are

- Geomorphology ("geo")
- Mean wave height ("wave")
- Coastal slope ("slp")
- Tidal range ("tidal")
- Relative sea level rise ("rsl")
- Shoreline displacement or, equally, erosion rate ("eros")

Each variable is captured as an individual field within the attribute table. To kickstart the model's operations, the DEM and shoreline data are sourced directly from their respective file paths (meaning they should be just hooked at the start point of the model). Figure 3 shows a flow chart of the methodology for the ModelBuilder model.

3.2.2 Shoreline resolution enhancement

To attain a high resolution, particularly when integrating the values of the slope, the shoreline polyline is subdivided into small segments through the "Split Line at Vertices" function, ensuring that the original attributes remain intact.

3.2.3 Slope variable computation

To attain a high resolution, particularly when integrating values of the slope, the shoreline polyline is subdivided into small segments through the "Split Line at Vertices" function, ensuring that the original attributes remain intact.

The conventional methodology for slope variable computation is automated as follows:

- **Conditional DEM Generation:** A conditional DEM, highlighting regions elevated above 5 m, is produced by using the "Con" tool.
- **DEM Conversion:** This conditional DEM is then converted into a polygon via the "Raster to Polygon" tool.
- **Correlation with the Shoreline:** Each shoreline segment's proximity to the nearest slope value in the conditional DEM polygon is computed by employing the "Near" tool. Subsequently, the "slope_rate" field is generated and populated by using the following formula in the "Calculate Field", where run is the result of near, and rise is 4:

$$\text{slope}(\%) = \frac{\text{rise}}{\text{run}} \times 100 \tag{2}$$

- **Normalization:** The z-score normalization technique is applied to the slope values. This method is preferred given the variable slope ranges across the extensive regions considered in general for CVI calculations. Normalization involves the calculation of the mean (μ) and standard deviation (σ). Thereafter, the normalized values (z-scores) are computed by using the following formulas in the "Calculate field":

$$\mu = \frac{1}{N} \tag{3}$$

$$\sigma = \sqrt{\frac{1}{N}\sum_{i=1}^{N}\left(x_i - \mu\right)^2} \tag{4}$$

$$2z = \frac{x - \mu}{\sigma} \tag{5}$$

3.2.4 Hybrid calculation of vulnerability

A hybrid approach determines the categorization of the

Figure 3 Visual representation of the ModelBuilder model constructed in ArcGIS software

slope's vulnerability. This method combines general standards (traditional categorization) (European Commission, 2004) with region-specific standards (statistical normalization), offering a comprehensive categorization system and ensuring that the vulnerability assessment is specific to the terrain and informed by the broader landscape context.

The hybrid classification method leverages the absolute values of the slope and their statistical standing within the dataset. The reasoning behind this approach is provided below:

• **Stability of Extremes**: Extremely steep or flat terrains inherently exhibit specific vulnerabilities. Steep terrains (> 12%) generally have low vulnerability to coastal issues, such as inundation, and are hence classified as "very low". Conversely, very flat terrains (< 3%) are highly susceptible, leading to a "very high" vulnerability classification.

• **Addressing the Middle Ground**: The vulnerability of slopes that are not at the extremes is not only dictated by their steepness, but also by how they compare with other slopes in the region as well. *z*-Score normalization becomes vital in this situation.

• **Statistical Significance of the *z*-Score**: *z*-Scores offer insights into how unusual or typical a slope is within the dataset. A positive *z*-score indicates that the slope is steeper than average, whereas a negative *z*-score means it is gentler than average. The closer the *z*-score is to 0, the closer the slope is to the mean value of the dataset.

• **Balancing Raw Values and Relative Standing**: By considering the actual value of the slope and its *z*-score (Table 2), the hybrid classification method ensures that slopes are not just evaluated in isolation but also in the context of their surroundings. For example, a slope that might be considered of "moderate" vulnerability in one region might be classified differently in another region where the average slope is steeper or gentler (Table 3).

Essentially, the hybrid table is a multiattribute table, and the results are obtained through decision making between the two integrated tables. This technique is called multiattribute decision making (MADM).

Table 2 Classification of vulnerability based on *z*-score normalized values

Classification of vulnerability	*z*-Score normalization
Very low (1)	>2
Low (2)	1–2
Moderate (3)	−1–1
High (4)	−2–−1
Very high (5)	<−2

Table 3 Hybrid calculation of vulnerability based on coastal slope (%) and *z*-score normalized values

Slope rate	Slope normalization	Classification of vulnerability
>12	Any	1
12–9	⩽0	2
12–9	>0	3
9–6	>0	4
9–6	<0	2
9–6	=0	3
6–3	⩾0	4
6–3	<0	3
<3	Any	5

3.2.5 Multi-attribute decision making (MADM)

MADM is a method used to evaluate and rank multiple alternatives on the basis of various criteria. It involves comparing different options by assigning values or weights to each criterion, ensuring a comprehensive assessment (Tzeng and Huang, 2011). Although numerous established popular MADM models exist, our model is simpler than others, using direct thresholds and *z*-score normalization to produce rankings.

• **Alternatives:** Different locations (lines) with specific slope values.

• **Criteria:** The value of the slope (quantitative) and its *z*-score normalization (statistical measure).

3.2.6 Final CVI calculation

The culminating step involves the generation and computation of the CVI field. The CVI is calculated by using the formula provided in the "Calculate Field" tool:

$$\mathrm{CVI} = \frac{1}{n}\sum_{i=1}^{n} p_{\mathrm{i}} \tag{6}$$

where n is the number of the parameters (n = 6 in our case), and p_{i} is the value of each parameter.

4 Results

Upon the creation of the ModelBuilder model, the CVI was calculated for the study area (Figure 4). Modeling results show that the CVI fluctuates between 2.3 and 7.3.

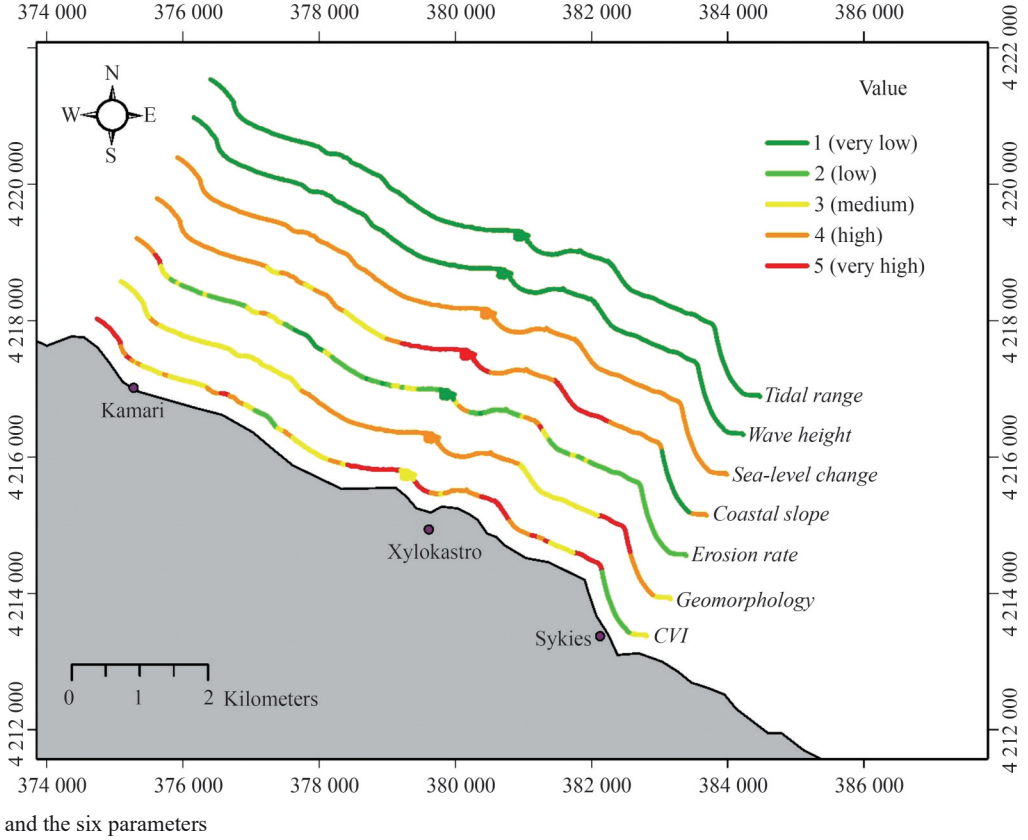

Figure 4 CVI and the six parameters

Similar to the parameters' values, the CVI is classified into ranges (i.e., medium for values between 3 and 4, high for values between 4 and 5, and very high for values greater than 5).

Given that coastal erosion is affected by multiple parameters, its assessment requires the weighting of these parameters in accordance with the study area (Li et al., 2015). Of the six parameters, sea level changes, wave height, and tidal range were considered equal for the whole study area and, therefore, bear no actual influence on the geographical distribution of the CVI values. Of course, we can speculate that each parameter has a different impact on each part of the coastline. However, due to the lack of detailed measures for these three parameters, we cannot further model their impact on our study area.

It is interesting to mention that there are only two distinct areas where the CVI is low; approximately half of the studied shoreline is of medium vulnerability, whereas the other half is of high to very high vulnerability. Except for the two small regions in Kamari and Sykia, where the CVI is very high, only the broader area of Xylokastro falls into the very high category; this finding is consistent with the published data on coastal erosion in this part (Valaouris et al., 2014; Vassilakis et al., 2016).

5 Discussion

5.1 Functionality of the ModelBuilder

Notable differences exist between the results of this study and those of previous works in the same area. These differences are mainly attributed to the fact that compared with the present work, all three previous studies on this area (Karymbalis et al., 2012; Ramnalis et al., 2023; Tragaki et al., 2018) focused on a larger area and therefore provided fewer details on the characteristics (predominantly geomorphology) of the study area.

Moreover, there is consistency with the situation reported by Karymbalis et al. (2012), i.e. that Kamari was characterized with medium vulnerability, which increased toward Sykia. The same trend was found by Ramnalis et al. (2023), who reported that coastal vulnerability ranged from low to high or medium to very high from Kamari to Sykia (depending on which of the two indices is used). Based on this situation, we conclude that coastal vulnerability in the central part of the study area between Kamari and Sykia exhibits an increasing tendency, while in the area of Sykia (i.e., from NW to SE), it remains low.

Some of the activities, such as the initial segmentation of the coastline based on geomorphology, were conducted manually. An automatization of this process would require multiple open datasets, which were unavailable in our case. Nevertheless, the rest of the processes were conducted automatically by using the ModelBuilder model. Therefore, the overall process of CVI calculation was time-saving. Moreover, the consistency between our results and those of previous works points to the fact that our ModelBuilder model functioned correctly.

5.2 Advantages and disadvantages of an automated process for CVI calculation

The CVI is a commonly used index for assessing coastal vulnerability and can be very efficient for coastal management (Loinenak et al., 2015; McLaughlin et al., 2010). It combines the coastal zone's sensitivity to sea level changes, which is reflected by its natural properties, such as morphological inclination and wave action, with its adaptability to potential changes. It has proven to be an effective way of estimating vulnerability to coastal hazards and understanding the effect of each social or physical parameter (Charuka et al., 2023). Another great advantage of the CVI is that, in contrast to a "physical" model of coastal vulnerability, it is dimensionless, meaning that it allows for comparisons between shorelines of different geological, geomorphological, and social configurations. Moreover, it can simplify parameters that would otherwise be a challenge to incorporate into a mathematical model (McLaughlin et al., 2010). For these reasons, the CVI is still used today despite being a relatively old methodological approach (e.g., Charuka et al., 2023; Depountis et al., 2023; Komi et al., 2022; Ramnalis et al., 2023; Roukounis and Tsihrintzis, 2022; Tsaimou et al., 2023).

We can enumerate some advantages and limitations of the technique based on ModelBuilder compared with the traditional method for calculating the CVI. These advantages and limitations are summarized in Table 4. To begin with, several functions cannot and should not be automated. The first is the segmentation of the coastline and its characterization based on the geomorphology parameter. Different authors have used different methods or a combination of different approaches to quantify this parameter. These approaches include the use of aerial photos (e.g., Charuka et al. 2023), geological maps (e.g., Ramnalis et al. 2023), or topographic maps and fieldwork (e.g., Ainee and Anwar 2014).

However, despite the technological advances for coastal studies, including GIS, remote sensing, and artificial intelligence (e.g., Bahari et al., 2023; Kumar et al., 2020), geomorphological mapping cannot be done purely automatically without fieldwork by experts (Hamidova et al., 2024). Coastal environments are no exception. While this situation may not be the case on large scales, the accuracy of an automated method lessens as the scale reduces (van der Meij et al., 2022).

For the parameter of geomorphology, a ModelBuilder model like the one proposed herein can be used. Nevertheless, the procedure will not be purely automated because it

Table 4 Major advantages and disadvantages of an automated method vs. a manual method for CVI calculation

Parameter	Automated method	Manual method
Time	(+) Time-saving	(−) Time-consuming
Error in the calculations	(+) Less feasible (done automatically)	(−) Highly feasible, especially in large areas
Accuracy of the final output	(+) Highly accurate, with accuracy proportional to the resolution of the data	(−) Accuracy is often limited deliberately because it would require extra time and effort
Application	(+) Can be applied simultaneously in different areas or in the same area under different conditions	(−) Must be made separately in each case without saving time
Modification	(−) Cannot be applied under a different CVI equation (e.g., a modified index)	(+) Once the CVI is calculated, a modified version can be calculated within a short time
Complete automatization	(−) The geomorphology factor and the thresholds of the other factors cannot be identified automatically	-

may still require some adjustments in accordance with the study area. For example, while the method of slope calculation is fixed, adjustments could be needed in accordance with the configuration of the study area. In addition, in the case that the three parameters we consider stable (wave height, tidal range, and sea level changes) do show some variation, their variation will differ from area to area, and modification and/or customization may be required (cf. Kaliraj and Chandrasekar, 2012). Our ModelBuilder model, of course, is created to be applied in areas wherein these three parameters will not be stable. In any case, work at the researcher level needs to be conducted in GIS and the field to produce accurate results.

Some of the benefits of the ModelBuilder model method over the purely manual method of CVI calculation must be noted. First, once all the data are imported into GIS, manual calculations require a large amount of time, which is dependent on the length of the studied shoreline, geomorphological characteristics (which determine the number and length of segments based on the geomorphology parameter), and characteristics of the other parameters. It involves the segmentation of the coastal zone and the designation of a vulnerability value for each segment. Furthermore, depending on the length of the studied coastline and the number of segments, mistakes are easy to make.

The ModelBuilder model that we developed ensures that some of the above procedures are conducted automatically in a short time and with the necessary accuracy. While the geomorphology parameter still has to be categorized manually, the other parameters can be categorized by the software. Vulnerability values are assigned automatically. In addition, the CVI itself is calculated automatically. The only procedures that must be conducted manually include setting the thresholds for sea level changes, wave height, tidal range (in case of variation), and shoreline displacement, i.e., which values will correspond to what vulnerability. However, these four parameters cannot be calculated purely automatically because they may differ from area to area.

It is also worth mentioning that several errors may arise while calculating the CVI manually, particularly in the case when the coastline is long or when a factor has numerous different characterizations along the coastline. For example, when dealing with a wavelength of considerable variation, the structured query language selection from the GIS may induce typographical errors, such as “2.5” instead of “2.0” or a multiplication sign instead of a division sign, and the user may not notice these errors. The nonmanual method calculates each factor and mathematical value automatically, thereby reducing the possibility of error substantially.

A further advantage of the automated process is that it can be applied simultaneously in different areas once the data are prepared. Moreover, the automated method can be applied successively in the same area but with different conditions (e.g., thresholds for the factors). This situation is not true for the manual method. An important disadvantage of the automated method is that once the factors have been categorized, a modified version of the CVI, such as one with the inclusion of another factor and/or the rejection of a pre-existing one, cannot be applied. This situation would require the development of a new ModelBuilder model.

Although the CVI is an index that is easy to calculate, needing simple GIS processes and data that are easy to find, it still requires considerable time to be properly and accurately calculated and attention to avoid potential mistakes. With ModelBuilder, many procedures can be automated or semiautomated (Kaliraj and Chandrasekar, 2012) such that the necessary time is reduced and potential human mistakes are avoided. We do believe that this model will help future studies by scientists and coastal authorities/stakeholders as both direct increasing attention to coastal zones.

A major advantage of a ModelBuilder model is that it depicts potentially complex functions and processes in the form of a simple and easy-to-follow flow chart. In this way, the creator of the model can easily monitor it, alter the order in which functions are performed, and identify

potential failures or function errors (Darwish, 2023; Deabes, 2017). Moreover, readers can better understand the methodology used. Another advantage is that it can link raster and vector files even into the same function if necessary (Chang, 2014). Moreover, all the files created in the intermediate processing are preserved and can be used or modified if necessary (Darwish, 2023).

5.3 Major limitations of the current study

It is crucial to refer to the major limitations that were faced during this study. To begin with, while various open sources of data concerning the maritime parameters of the Greek coastline (in our case, significant wave heights and tidal range) exist, they concern the whole Greek coastline or massive segments of it. As a result, their accuracy is questionable when small scales are considered. An example is the significant wave height of our study area, which is 0–0.1 m (and is the same throughout the whole northeastern part of the Peloponnese). Field observations during previous studies on this location have confirmed that the significant wave height is indeed low. However, the value of 0.1 m found in the literature (Soukissian et al., 2007) is low for this area, given its problem with coastal erosion (Valaouris et al., 2014; Vassilakis et al., 2016).

A similar problem is found for relative sea level changes. On large scales, e.g., on the scale of the whole Corinthian Gulf, a relatively accurate classification of the coastline based on this factor would be possible on the basis of the data provided by the literature (cf. Evelpidou et al. (2023) and references within). However, on small scales, like our case study, identifying segments of different tectonic activities is difficult mainly because first, tectonic activity has been identified in different ways by each researcher. Ostensive indicators of tectonic uplift or subsidence include landforms (marine terraces, tidal notches, and beach rocks), archaeological finds (e.g., submerged ancient buildings and uplifted harbors), geodetic data, and fault activity. Therefore, even when authors provide quantitative data on vertical tectonic movements, homogenizing and comparing them are difficult. Second, measuring considerable differences in vertical tectonic movements along very small stretches of coastline is difficult unless substantially different events have indeed occurred or differential movements are present.

In numerous surveys, the geological parameters of the CVI are often weighted more than the physical (oceanographical) ones, usually due to a lack of data. However, climate change has already led to remarkable changes in marine parameters, and this situation has exerted a substantial impact on many coasts. As a consequence, marine parameters are crucial and should not be neglected (Pang et al., 2023).

In such cases, identifying these parameters through *in situ* observations and measurements in addition to the data from the literature would be best. An even more accurate way of quantifying wave activity is through hydrodynamic models (Pang et al., 2023). Of course, this work did not conduct this approach because it does not aim to identify the coastal vulnerability of the area and provide accurate quantitative results but rather aims to automatize coastal vulnerability assessment. Clearly, to be integrated, this assessment must be accompanied by field observations and extensive pre-GIS work. Therefore, an automatization of CVI calculation is important.

6 Conclusions

This study shows that even though not all processes could be automated (and should not be automated but should instead be determined and manually inserted by researchers), ModelBuilder is a highly valuable tool, not only for calculating the CVI but for modeling all of its parameters as well. For example, the segmentation of the shoreline based on geomorphology cannot be automated because it is determined by the study area and the researchers' experience. By contrast, its resegmentation based on other parameters was facilitated by ModelBuilder, accelerating the process and minimizing the possibility of mistakes. The ModelBuilder model facilitates the error-free assignment of the parameters' values. It needs to be applied in other coastal areas for testing and assessment. This work's specific study area is at high risk because its CVI values are high to very high in most parts and moderate in others. This result is consistent with the findings of already existing works in the study area, confirming that the ModelBuilder has functioned well.

Competing interest The authors have no competing interests to declare that are relevant to the content of this article.

References

AbdelRahman MAE, Tahoun S (2019) GIS model-builder based on comprehensive geostatistical approach to assess soil quality. Remote Sens Appl Soc Environ 13: 204-214. https://doi.org/10.1016/j.rsase.2018.10.012

Ahmed A, Nawaz R, Drake F, Woulds C (2018) Modelling land susceptibility to erosion in the coastal area of Bangladesh: A geospatial approach. Geomorphology 320: 82-97. https://doi.org/10.1016/j.geomorph.2018.08.004

Ainee GJ, Anwar AM (2014) Towards the implementation of continuous coastal vulnerability index in Malaysia: A review. J Teknol 71: 4. https://doi.org/10.11113/jt.v71.3819

Alexandrakis G, Karditsa A, Poulos S, Ghionis G, Kampanis N (2010) An Assessment of the Vulnerability to Erosion of the Coastal Zone Due to a Potential Rise of Sea Level: The Case of the Hellenic Aegean Coast-. Encycl Life Support Syst 3 16: 1951-1962. https://doi.org/10.1007/s10113-014-0730-9

Allen DW (2011) Getting to know ArcGIS modelBuilder. Esri Press

Anfuso G, Postacchini M, Di Luccio D, Benassai G (2021) Coastal sensitivity/vulnerability characterization and adaptation strategies: A review. J Mar Sci Eng 9: 72. https://doi.org/10.3390/jmse9010072

Ankrah J, Monteiro A, Madureira H (2023) Shoreline change and coastal erosion in west Africa: a systematic review of research progress and policy recommendation. Geosciences 13: 59. https://doi.org/10.3390/geosciences13020059

Armijo R, Meyer B, King GCP, Rigo A, Papanastassiou D (1996) Quaternary evolution of the Corinth Rift and its implications for the Late Cenozoic evolution of the Aegean. Geophys J Int 126: 11-53. https://doi.org/10.1111/j.1365-246X.1996.tb05264.x

Bagheri M, Ibrahim ZZ, Mansor S, Abd Manaf L, Akhir M F, Talaat W I A W, Wolf I (2023) Hazard assessment and modeling of erosion and sea level rise under global climate change conditions for coastal city management 04022038. Nat Hazards Rev 24. https://doi.org/10.1061/(ASCE)NH.1527-6996.0000593

Bahari NAABS, Ahmed AN, Chong KL, Lai V, Huang YF, Koo CH, Lin NgJ, El-Shafie A (2023) Predicting sea level rise using artificial intelligence: a review. Arch Comput Methods Eng 30: 4045-4062. https://doi.org/10.1007/s11831-023-09934-9

Barrantes-Castillo G, Ortega-Otárola K (2023) Coastal erosion and accretion on the Caribbean coastline of Costa Rica long-term observations. J South Am Earth Sci 127: 104371. https://doi.org/10.1016/j.ocecoaman.2023.106605

Belal AA, El-Ramady HR, Mohamed ES, Saleh AM (2014) Drought risk assessment using remote sensing and GIS techniques. Arab J Geosci 7: 35-53. https://doi.org/10.1007/s12517-012-0707-2

Briole P, Rigo A, Lyon-Caen H, Ruegg JC, Papazissi K, Mitsakaki C, Balodimou A, Veis G, Hatzfeld D, Deschamps, A (2000) Active deformation of the Corinth rift, Greece: results from repeated global positioning system surveys between 1990 and 1995. J Geophys Res 105: 25605-25625. http://doi.org/10.1029/2000JB900148

Buhmann E, Nothhelfer U, Pietsch M (2002) Trends in GIS and visualization in environmental planning and design. In: Proceedings at Anhalt University. Wichmann, Heidelberg, Germany, p 192

Castelle B, Kras E, Masselink G, Scott T, Konstantinou A, Luijendijk A (2024) Satellite-derived sandy shoreline trends and interannual variability along the Atlantic coast of Europe. Sci Rep 14: 13002. https://doi.org/10.1038/s41598-024-63849-4

Celata F, Gioia E (2024) Resist or retreat? beach erosion and the climate crisis in Italy: scenarios, impacts and challenges. Appl Geogr 169: 103335. https://doi.org/10.1016/j.apgeog.2024.103335

Chaaban F, Darwishe H, Battiau-Queney Y, Louche B, Masson E, El Khattabi, J, Carlier E (2012) Using ArcGIS® modelbuilder and aerial photographs to measure coastline retreat and advance: North of France. J Coast Res 28: 1567-1579. https://doi.org/10.2112/JCOASTRES-D-11-00054.1

Chadenas C, Chotard M, Navarro O, Kerguillec R, Robin M, Juigner M (2023) Coastal erosion risk: population adaptation to climate Change—A case study of the pays de la Loire Coastline. Weather Clim Soc 15: 145-157. https://doi.org/10.1175/WCAS-D-22-0011.1

Chang K (2014) Introduction to geographic information systems, 7th edn. McGraw-Hill, Boston, U.S.A

Charuka B, Angnuureng DB, Brempong EK, Agblorti SKM, Antwi Agyakwa KT (2023) Assessment of the integrated coastal vulnerability index of Ghana toward future coastal infrastructure investment plans. Ocean Coast Manag 244: 106804. https://doi.org/10.1016/j.ocecoaman.2023.106804

Church JA, White NJ (2011) Sea-Level Rise from the Late 19th to the Early 21st Century. Surv Geophys 32: 585-602. https://doi.org/10.1007/s10712-011-9119-1

Copernicus (2023) Copernicus Marine Data Store. https://data.marine.copernicus.eu/products. Accessed 8 Dec 2023

Csáfordi P, Podör A, Bug J, Gribovszki Z (2012) Soil erosion analysis in a small forested catchment supported by ArcGIS model builder. Acta Silv Lignaria Hungarica 8: 39-55. https://doi.org/10.2478/v10303-012-0004-5

Dada OA, Almar R, Morand P (2024) Coastal vulnerability assessment of the West African coast to flooding and erosion. Sci Rep 14: 890. https://doi.org/10.1038/s41598-023-48612-5

Darwish KS (2023) GIS-Based spatial modeling of potential impacts of sea level rise along the nile delta coast. In: Darwish KS (ed) Hazard Modeling and Assessment of the Nile Delta Coast, 1st edn. Springer, Cham, Switzerland, pp 129-180. https://doi.org/10.1007/978-3-031-44324-4_4

Deabes EA (2017) Applying ArcGIS to estimate the rates of shoreline and back-shore area changes along the Nile delta coast, Egypt. Int J Geosci 8: 332-348. https://doi.org/10.4236/ijg.2017.83017

Depountis N, Apostolopoulos D, Boumpoulis V, Christodoulou D, Dimas A, Fakiris E, Leftheriotis G, Menegatos A, Nikolakopoulos K, Papatheodorou G, Sabatakakis N (2023) Coastal erosion identification and monitoring in the patras gulf (Greece) Using multi-discipline approaches. J Mar Sci Eng 11: 654. https://doi.org/10.3390/jmse11030654

Diez PG, Perillo GME, Piccolo MC (2007) Vulnerability to sea-level rise on the coast of the Buenos Aires Province. J Coast Res 23: 119-142. https://doi.org/10.2112/04-0205.1

Dike EC, Amaechi CV, Beddu SB, Weje II, Ameme BG, Efeovbokhan O, Oyetunji AK (2024) Coastal vulnerability index sensitivity to shoreline position and coastal elevation parameters in the Niger Delta region, Nigeria. Sci Total Environ 919: 170830

Dong WS, Ismailluddin A, Yun LS, Ariffin EH, Saengsupavanich C, Abdul Maulud KN, Ramli MZ, Miskon MF, Jeofry MH, MJ, Mohd FA, Hamzah SB, Yunus K (2024) The impact of climate change on coastal erosion in Southeast Asia and the compelling need to establish robust adaptation strategies. Heliyon 10: e25609. https://doi.org/10.1016/j.heliyon.2024.e25609

Doukakis E (2005) Coastal vulnerability and risk parameters. Eur Water 11/12: 3-7

Dronkers J (2005) Dynamics of coastal systems. World Scientific Publishing Compan, Hackensack, New Jersey, U. S. A. 450 pp. https://doi.org/10.1142/5781. 1st ed

Effat HA (2017) Mapping potential wind energy zones in Suez Canal region, using satellite data and spatial multicriteria decision models. J Geosci Environ Prot 5: 46-61. https://doi.org/10.4236/gep. 2017.510005

Effat HA, El-Zeiny A (2017) Modeling potential zones for solar energy in Fayoum, Egypt, using satellite and spatial data. Model Earth Syst Environ 3: 1529-1542. https://doi.org/10.1007/s40808-017-0372-2

ESRI (2024) What is ModelBuilder? https://pro.arcgis.com/en/pro-app/latest/help/analysis/geoprocessing/modelbuilder/what-is-modelbuilder-. htm. Accessed 17 Jul 2024

European Commission (2004) Living with coastal erosion in Europe. Office for Official Publications of the European Communities, the Netherlands

Evelpidou N, Ganas A, Karkani A, Spyrou E, Saitis G (2023) Late quaternary relative sea-level changes and vertical GNSS motions in the gulf of corinth: The Asymmetric Localization of Deformation Inside an Active Half-Graben. Geosciences 13: 329. https://doi.org/10.3390/geosciences13110329

Evelpidou N, Tzouxanioti M, Liaskos A (2022) Coastal erosion: The future of sandy beaches. In: Proceedings of the European Academy of Sciences & Arts. pp 1-16. https://doi.org/10.4081/peasa.12

Fok H (2012) Ocean Tides Modeling Using Satellite Altimetry. Ph.D. thesis, Ohio State University

Garola A, López-Dóriga U, Jiménez JA (2022) The economic impact of sea level rise-induced decrease in the carrying capacity of Catalan beaches (NW Mediterranean, Spain). Ocean Coast Manag 218: 106034

Garzo PA, Sánchez-Caro, Mojica M (2023) Coastal erosion in temperate barriers: an anthropized sandy beach in Buenos Aires, Argentina. J South Am Earth Sci 128: 104453. https://doi.org/10.1016/j.jsames.2023.104453

Ghanavati M, Young I, Kirezci E, Ranasinghe R, Duong TM, Luijendijk AP (2023) An assessment of whether long-term global changes in waves and storm surges have impacted global coastlines. Sci Rep 13: 11549. https://doi.org/10.1038/s41598-023-38729-y

González Rodríguez SV, Negro Valdecantos V, del Campo JM, Torrodero Numpaque V (2024) Comparing the effects of erosion and accretion along the eastern coast of Río de Janeiro and Guanabara bay in Brazil. Sustainability 16: 5728. https://doi.org/10.3390/su16135728

Goodchild MF (2005) GIS, spatial analysis and modeling overview. In: Maguire B, Goodchild MF (eds) GIS, Spatial Analysis, and Modeling. ESRI, Redlands, California, U.S.A., pp 1-18

Gornitz V, White TW, Cushman RM (1991) Vulnerability of the US to future sea level rise. In: 7th Symposium on Coastal and Ocean Management, 8-12 July 1991. Oak Ridge National Laboratory, Long Beach, California, U.S.A

Gracia A, Rangel-Buitrago N, Oakley JA, Williams AT (2018) Use of ecosystems in coastal erosion management. Ocean Coast Manag 156: 277-289. https://doi.org/10.1016/j.ocecoaman.2017.07.009

Hamid AIA, Din AHM, Abdullah NM, Yusof N, Hamid MRA, Shah AM (2021) Exploring space geodetic technology for physical coastal vulnerability index and management strategies: A review. Ocean Coast Manag 214: 105916. https://doi.org/10.1016/j.ocecoaman.2021.105916

Hamidova E, Bosino A, Franceschi L (2024) Nature-based solution integration to enhance urban geomorphological mapping: a methodological approach. Land 13: 467. https://doi.org/10.3390/land13040467

Hellenic Cadastre (2021) Viewing of Orthophotos. https://gis.ktimanet.gr/wms/ktbasemap/default.aspx. Accessed 21 Apr 2024

Hellenic Navy Hydrographic Service (2020) National Tide Gauge Network. https://www.hnhs.gr/el/online/2015-05-16-18-51-00. Accessed 8 Dec 2023

Hofstede JL (2024) Status and prospects of nature-based solutions for coastal flood and erosion risk management in the Federal State of Schleswig–Holstein, Germany. J Coast Conserv 28: 40. https://doi.org/10.1007/s11852-024-01042-5

Hollenstein C, Müller MD, Geiger A, Kahle HG (2008) Crustal motion and deformation in Greece from a decade of GPS measurements, 1993-2003. Tectonophysics 449: 17-40. https://doi.org/10.1016/j.tecto.2007.12.006

Hydrographic Service of the Hellenic Navy (2005) Tides of the Greek Ports, publication of hellenic navy hydrographic service. Publication of the Hydrographic Service of the Hellenic Navy, Athens, Greece

Hysa A, Baskaya FAT (2018) A GIS-based method for revealing the transversal continuum of natural landscapes in the coastal zone. Methods 5: 514-523. https://doi.org/10.1016/j.mex.2018.05.012

Israel Marine Data Center Mediterranean Wave Forecast (WAM). https://israмar.ocean.org.il/isramar2009/wave_model/default.aspx?model=wam. Accessed 8 Dec 2023

Jana A, Bhattacharya AK (2013) Assessment of coastal erosion vulnerability around midnapur-balasore coast, Eastern India using Integrated Remote Sensing and GIS Techniques. J Indian Soc Remote Sens 41: 675-686. https://doi.org/10.1007/s12524-012-0251-2

Jevrejeva S, Williams J, Vousdoukas MI, Jackson LP (2023) Future sea level rise dominates changes in worst case extreme sea levels along the global coastline by 2100. Environ Res Lett 18: 024037. https://doi.org/10.1088/1748-9326/acb504

Kaliraj S, Chandrasekar N (2012) Geo-processing model on coastal Vulnerability Index to Explore Risk Zone along the South West Coast of Tamilnadu, India. Int J Earth Sci Eng 5: 1138-1147

Kantamaneni K, Rice L, Du X, Allali B, Yenneti K (2022) Are current UK coastal defences good enough for tomorrow? An assessment of vulnerability to coastal erosion. Coast Manag 50: 142-159. https://doi.org/10.1080/08920753.2022.2022971

Karymbalis E, Chalkias C, Chalkias G, Grigoropoulou E, Manthos G, Ferentinou M (2012) Assessment of the sensitivity of the southern coast of the Gulf of Corinth (Peloponnese, Greece) to sea-level rise. Cent Eur J Geosci 4: 561-577. https://doi.org/10.2478/s13533-012-0101-3

Kirezci E, Young IR, Ranasinghe R, Lincke D, Hinkel J (2023) Global-scale analysis of socioeconomic impacts of coastal flooding over the 21st century. Front Mar Sci 9: 1024111. https://doi.org/10.3389/fmars.2022.1024111

Komi A, Petropoulos A, Evelpidou N, Poulos S, Kapsimalis V (2022) Coastal vulnerability assessment for future sea level rise and a comparative study of two pocket beaches in seasonal scale, Ios Island, Cyclades, Greece. J Mar Sci Eng 10: 1673. https://doi.org/10.3390/jmse10111673

Koroglu A, Ranasinghe R, Jiménez JA, Dastgheib A (2019) Comparison of coastal vulnerability index applications for Barcelona Province. Ocean Coast Manag 178: 104799. https://doi.org/10.1016/j.ocecoaman.2019.05.001

Kumar L, Afzal MS, Afzal MM (2020) Mapping shoreline change using machine learning: a case study from the eastern Indian coast. Acta Geophys 68: 1127-1143. https://doi.org/10.1007/s11600-020-00454-9

Lam NSN, Xu YJ, Liu KB, Dismukes DE, Reams M, Pace RK, Qiang YI, Narra S, Li K, Bianchette TA, Cai H, Zou L, Mihunov V (2018) Understanding the Mississippi River delta as a coupled natural-human system: Research methods, challenges, and prospects. Water 10: 1054. https://doi.org/10.3390/w10081054

Li X, Zhou Y, Tian B, Kuang R, Wang L (2015) GIS-based methodology for erosion risk assessment of the muddy coast in the Yangtze Delta. Ocean Coast Manag 108: 97-108. https://doi.org/10.1016/j.ocecoaman.2014.09.028

Liu Y, Zhang Y (2023) Assessment of Coastal Zone Vulnerability in the Context of Sea Level Rise and Climate Change. In: Nhantumbo BJ, Dada OA, Ghomsi FEK (eds) Sea Level Rise and Climate Change–Impacts on Coastal Systems and Cities. IntechOpen, pp 1-19

Loinenak FA, Hartoko A, Muskananfola MR (2015) Mapping of coastal vulnerability using the coastal vulnerability index and geographic information system. Int J Technol 5: 819-827. https://doi.org/10.14716/ijtech.v6i5.1361

Maanan M, Maanan M, Rueff H, Adouk N, Zourarah B, Rhinane H (2018) Assess the human and environmental vulnerability for coastal hazard by using a multi-criteria decision analysis. Hum

Ecol Risk Assess 24: 1642-1658. https://doi.org/10.1080/10807039.2017.1421452

MacManus K, Balk D, Engin H, McGranahan G, Inman R (2021) Estimating population and urban areas at risk of coastal hazards, 1990–2015: how data choices matter. Earth Syst Sci Data 13: 5747-5801. https://doi.org/10.5194/essd-13-5747-2021

Maguire D, Batty M, Goodchild MF (2005) GIS, Spatial Analysis, and Modeling. ESRI, Redlands, California, U.S.A

McLaughlin S, Andrew J, Cooper G (2010) A multi-scale coastal vulnerability index: A tool for coastal managers? Environ Hazards 9: 233-248. https://doi.org/10.3763/ehaz.2010.0052

Merlotto A, Bértola GR, Piccolo MC (2016) Hazard, vulnerability and coastal erosion risk assessment in Necochea Municipality, Buenos Aires Province, Argentina. J Coast Conserv 20: 351-362. https://doi.org/10.1007/s11852-016-0447-7

Mohamed ES, Belal A, Shalaby A (2015) Impacts of soil sealing on potential agriculture in Egypt using remote sensing and GIS techniques. Eurasian Soil Sci 48: 1159-1169. https://doi.org/10.1134/S1064229315100075

Mohamed ES, Morgun EG, Goma Bothina SM (2011) Assessment of soil salinity in the Eastern Nile Delta (Egypt) using geoinformation techniques. Moscow Univ Soil Sci Bull 66: 11-14. https://doi.org/10.3103/s0147687411010030

Mohanty PC, Mahendra RS, Nayak RK, Kumar TS (2017) Impact of sea level rise and coastal slope on shoreline change along the Indian coast. Nat Hazards 89: 1227-1238. https://doi.org/10.1007/s11069-017-3018-9

Mohd FA, Abdul Maulud KN, Karim OA, Begum RA, Awang, NA, Ahmad A, Wan Mohamed A, Kamarudin MKA, Jaafar M, Wan Mohtar WHa Melini (2019) Comprehensive coastal vulnerability assessment and adaptation for Cherating-Pekan coast, Pahang, Malaysia. Ocean Coast Manag 182: 104948. https://doi.org/10.1016/j.ocecoaman.2019.104948

Moradi M, Chertouk N, Ilinca A (2022) Modelling of a wave energy converter impact on coastal erosion, a case study for Palm Beach-Azur, Algeria. Sustainability 14: 16595. https://doi.org/10.3390/su142416595

Mugnier C (2002) Grids and datums: the hellenic republic. photogramm eng remote sens 68: 1237-1238

Mullick MRA, Islam KMA, Tanim AH (2020) Shoreline change assessment using geospatial tools: a study on the Ganges deltaic coast of Bangladesh. Earth Sci Informatics 13: 299-316. https://doi.org/10.1007/s12145-019-00423-x

Narra P, Coelho C, Sancho F, Palalane J (2017) CERA: An open-source tool for coastal erosion risk assessment. Ocean Coast Manag 142: 1-14. https://doi.org/10.1016/j.ocecoaman.2017.03.013

National and Kapodistrian University of Athens (2023) Forecast Maps. https://forecast.uoa.gr/en/#. Accessed 8 Dec 2023

National Oceanography Centre (2023) Obtaining Tide Gauge Data. https://noc.ac.uk/. Accessed 8 Dec 2023

Pang T, Wang X, Nawaz RA, Keefe G, Adekanmbi T (2023) Coastal erosion and climate change: A review on coastal-change process and modeling. Ambio 52: 2034-2052. https://doi.org/10.1007/s13280-023-01901-9

Patra A, Dodet G, Accensi M (2023) Historical global ocean wave data simulated with CMIP6 anthropogenic and natural forcings. Sci Data 10: 325. https://doi.org/10.1038/s41597-023-02228-6

Pendleton EA, Thieler ER, Williams SJ (2005) Coastal vulnerability assessment of golden gate national recreation area to sea-level rise. US Geological Survey, Woods Hole, Massachusetts, U.S.A

Pendleton EA, Thieler ER, Williams SJ (2010) Importance of coastal change variables in determining vulnerability to sea- and lake-level change. J Coast Res 26: 176-183. https://doi.org/10.2112/08-1102.1

Pfaff RM, Glennon JA (2004) Building a groundwater protection model. In: ArcUser July-September 2004. pp 54-59

Pirazzoli PA, Stiros SC, Arnold M, Laborel J, Laborel-Deguen F, Papageorgiou S (1994) Episodic uplift deduced from Holocene shorelines in the Perachora Peninsula, Corinth area, Greece. Tectonophysics 229: 201-209. https://doi.org/10.1016/0040-1951(94)90029-9

Pouye I, Adjoussi DP, Ndione JA, Sall A (2024) Evaluation of the Economic Impact of Coastal Erosion in Dakar Region. J Coast Res 40: 193-209. https://doi.org/10.2112/JCOASTRES-D-23-00018.1

Ramieri E, Hartley AJ, Barbanti A, Santos FD, Gomes A, Hilden M, Laihonen P, Marinova N, Santini M (2011) Methods for assessing coastal vulnerability to climate change. ETC CCA Technical Paper 1/2011, European Topic Centre on Climate Change Impacts, Vulnerability and Adaptation, European Environment Agency. 93 pp

Ramnalis P, Batzakis DV, Karymbalis E (2023) Applying two methodologies of an integrated coastal vulnerability index (Icvi) To Future Sea-Level Rise. Case Study: Southern Coast of the Gulf of Corinth, Greece. Geoadria 28: 7-24. https://doi.org/10.15291/geoadria.4046

Roberts GP, Houghton SL, Underwood C, Papanikolaou I, Cowie PA, Van Calsteren P, Wigley T, Cooper FJ, McArthur JM (2009) Localization of quaternary slip rates in an active rift in 105 years: An example from central Greece constrained by 234U-230Th coral dates from uplifted paleoshorelines. J Geophys Res 114: B10406. https://doi.org/10.1029/2008JB005818

Roukounis CN, Tsihrintzis VA (2022) Indices of coastal vulnerability to climate change: a Review. Environ Process 9: 29. https://doi.org/10.1007/s40710-022-00577-9

Roukounis CN, Tsoukala VK, Tsihrintzis VA (2023) An index-based method to assess the resilience of urban areas to coastal Flooding: The Case of Attica, Greece. J Mar Sci Eng 11: 1776. https://doi.org/10.3390/jmse11091776

Saengsupavanich C, Ratnayake AS, Yun LS, Ariffin EH (2023) Current challenges in coastal erosion management for southern Asian regions: examples from Thailand, Malaysia, and Sri Lanka. Anthr Coasts 6: 15. https://doi.org/10.1007/s44218-023-00030-w

Saleh AM, Belal AB, Mohamed ES (2015) Land resources assessment of El-Galaba basin, South Egypt for the potentiality of agriculture expansion using remote sensing and GIS techniques. Egypt J Remote Sens Sp Sci 18: S19-S30. https://doi.org/10.1016/j.ejrs.2015.06.006

Sánchez-Artús X, Gracia V, Espino M, Sierra JP, Pinyol J, Sánchez-Arcilla A (2023) Present and future flooding and erosion along the NW Spanish Mediterranean Coast. Front Mar Sci 10: 1125138. https://doi.org/10.3389/fmars.2023.1125138

Sarr MA, Pouye I, Sene A, Aniel-Quiroga I, Diouf AA, Samb F, Ndiaye ML, Sall M (2024) Monitoring and Forecasting of Coastal Erosion in the Context of Climate Change in Saint Louis (Senegal). Geographies 4: 287-303. https://doi.org/10.3390/geographies4020017

Schaller J, Mattos C (2010) ArcGIS ModelBuilder applications for landscape development planning in the Region of Munich, Bavaria. Digit Landsc Archit 1-12

Schuller E (2023) Sea level rise and coastal erosion in the United States. Symposium 37 Student Research & Creative Works Symposium, May 10, 2023, Easter Washington University, U.S.A. https://dc.ewu.edu/srcw_2023/res_2023/p2_2023/37

Setyawan WB (2022) Adaptation strategy to coastal erosion by rural communities: Lessons learned from Ujunggebang village, Indramayu, West Java, Indonesia. Marit Technol Res 4: 252846. https://doi.org/10.33175/mtr.2022.252846

Soukissian T, Hatzinaki M, Korres G, Papadopoulos A, Kallos G, Anadranistakis E (2007) Wind and wave atlas of the Hellenic seas. Hellenic Centre for Marine Research, Anavyssos, Greece (In Greek)

Stockdon HF, Palmsten ML, Doran KS, Long JW, Van der Westhuysen A, Snell RJ (2023) Operational forecasts of wave-driven water levels and coastal hazards for US Gulf and Atlantic coasts. Commun Earth Environ 4: 169. https://doi.org/10.1038/s43247-023-00817-2

Suhana MP, Nurjaya IW, Natih NMN (2016) Analisis kerentanan pantai timur pulau Bintan menggunakan digital shoreline analysis dan coastal vulnerability index. J Teknol Perikan dan Kelaut 7: 21-38. https://doi.org/10.24319/jtpk.7.21-38

Tadesse MG, Wahl T, Rashid MM, Dangendorf S, Rodríguez-Enríquez A, Talke SA (2022) Long-term trends in storm surge climate derived from an ensemble of global surge reconstructions. Sci Rep 12: 13307. https://doi.org/10.1038/s41598-022-17099-x

Tarigan TA, Ahmad AL, Fauzi MAR, Fatkhurrozi M (2024) Assessment of coastal vulnerability index (CVI) and its application along the Sragi Coast, South Lampung, Indonesia. GEOMATE J 26: 134-141

Thakur DA, Mohanty MP (2023) A synergistic approach towards understanding flood risks over coastal multi-hazard environments: Appraisal of bivariate flood risk mapping through flood hazard, and socio-economic-cum-physical vulnerability dimensions. Sci Total Environ 901: 166423. https://doi.org/10.1016/j.scitotenv.2023.166423

Thieler ER, Hammar-Klose ES (1999) National assessment of coastal vulnerability to sea-level rise, U.S. Atlantic Coast. USGS, Reston, Virginia, U.S.A

Thieler ER, Himmelstoss E, Zichichi J, Ergul A (2009) Digital shoreline analysis system (DSAS) version 4.3-an ArcGIS extension for calculating shoreline change. U.S. Geological Survey

Tiwari A, Ajmera S (2021) Land suitability assessment for agriculture using analytical hierarchy process and weighted overlay analysis in ArcGIS ModelBuilder. In: Recent Trends in Civil Engineering: Select Proceedings of ICRTICE 2019. Springer, Singapore, pp 735-762

Tragaki A, Gallousi C, Karymbalis E (2018) Coastal hazard vulnerability assessment based on geomorphic, oceanographic and demographic parameters: The case of the Peloponnese (Southern Greece). Land 7: 56. https://doi.org/10.3390/land7020056

Tsaimou CN, Papadimitriou A, Chalastani VI, Sartampakos P, Chondros M, Tsoukala VK (2023) Impact of spatial segmentation on the assessment of coastal vulnerability—Insights and Practical Recommendations. J Mar Sci Eng 11: 1675. https://doi.org/10.3390/jmse11091675

Tsimplis MN (1994) Tidal oscillations in the aegean and ionian seas. Estuar Coast Shelf Sci 39: 201-208

Tsokos A (2024) Coastal zone management in areas under the influence of geodynamic phenomena. Doctoral thesis, Department of Geology and Geoenvironment, National and Kapodistrian University of Athens, Athens, Greece

Turner JA, Leeder MR, Andrews JE, Rowe PJ, van Calsteren PV, Thomas L (2010) Testing rival tectonic uplift models for the Lechaion Gulf in the Gulf of Corinth rift. J Geol Soc London 167: 1237-1250. https://doi.org/10.1144/0016-76492010-035

Tzeng GH, Huang JJ (2011) Multiple attribute decision making: methods and applications. CRC Press, Boca Raton, Florida, U.S.A. & London, U.K. & New York, U.S.A

Uda T (2022) Fundamental issues in Japan's coastal management system for the prevention of beach erosion. Marit Technol Res 4: 251788. https://doi.org/10.33175/mtr.2022.251788

UNESCO (2023) Sea level station monitoring facility. http://www.ioc-sealevelmonitoring.org/map.php. Accessed 8 Dec 2023

Valaouris A, Poulos S, Petrakis S, Alexandrakis G, Vassilakis E, Ghionis G (2014) Processes affecting recent and future morphological evolution of the Xylokastro beach zone (Gulf of Corinth, Greece). Glob NEST J 16: 773-786. https://doi.org/10.30955/gnj.001254

van der Meij WM, Meijles EW, Marcos D, Harkema TTL, Candel JHJ, Maas GJ (2022) Comparing geomorphological maps made manually and by deep learning. Earth Surf Process Landforms 47: 1089-1107. https://doi.org/10.1002/esp.5305

Vassilakis E, Papadopoulou-Vrynioti K (2014) Quantification of deltaic coastal zone change based on multi-Temporal high resolution earth observation techniques. ISPRS Int J Geo-Information 3: 18-28. https://doi.org/10.3390/ijgi3010018

Vassilakis E, Skourtsos E, Kranis H (2007) Combination of morphometric indices as a method for the quantification of neotectonic evolution in active areas. In: 16th DRT Conference. Rendiconti della Società Geologica Italiana, Milan, Italy, p 214

Vassilakis E, Tsokos A, Kotsi E (2016) Shoreline change detection and coastal erosion monitoring using digital processing of a time series of high spatial resolution remote sensing data. Bull Geol Soc Greece 50: 1747-1755. https://doi.org/10.12681/bgsg.11898

Vernimmen R, Hooijer A (2023) New LiDAR-based elevation model shows greatest increase in global coastal exposure to flooding to be caused by early-stage sea-level rise. Earth's Futur 11: e2022EF002880. https://doi.org/10.1029/2022EF002880

Vousdoukas MI, Ranasinghe R, Mentaschi L, Plomaritis TA, Athanasiou P, Luijendijk A, Feyen L (2020) Sandy coastlines under threat of erosion. Nat Clim Chang 10: 260-263. https://doi.org/10.1038/s41558-020-0697-0

Winckler P, Martín RA, Esparza C, Melo O, Sactic MI, Martínez C (2023) Projections of beach erosion and associated costs in Chile. Sustainability 15: 5883. https://doi.org/10.3390/su15075883

Wischmeier WH, Smith DD (1978) Predicting rainfall erosion losses–A guide to conservation planning. In: Series: Agriculture Handbook 537: 3-4. USDA, Washington D.C., U.S.A